ORIGINAL PAPER

Bamboo shoot skin: turning waste to a valuable adsorbent for the removal of cationic dye from aqueous solution

Lin Zhu[1] · Penghui Zhu[1] · Liangjun You[1] · Songjun Li[1]

Abstract

The successful utilization of adsorption methods in the dye wastewater treatment had promoted us to develop inexpensive adsorbents from industrial and agricultural wastes. The work appraised the application potentiality of bamboo shoot skin (BSS) as an adsorbent. Batch adsorption of methylene blue (MB) was conducted to investigate the influence of the dosage of adsorbent, concentration of MB, time of adsorption, temperature, and initial pH value on the adsorption properties of BSS. Four frequently used adsorption kinetic models were utilized to fit the experimental results, and the pseudo-second-order kinetic model with big correlation coefficient could well describe the adsorption kinetics. The experimental equilibrium data were fitted by two frequently used adsorption isotherm models, and the Langmuir isotherm model described well. Its maximum adsorption capacity was 29.88 mg/g. The obtained thermodynamic parameters indicated that the adsorption process was spontaneous and exothermic in nature. In addition, the adsorption mechanism and comparison of BSS with other adsorbents were also discussed.

Graphical abstract
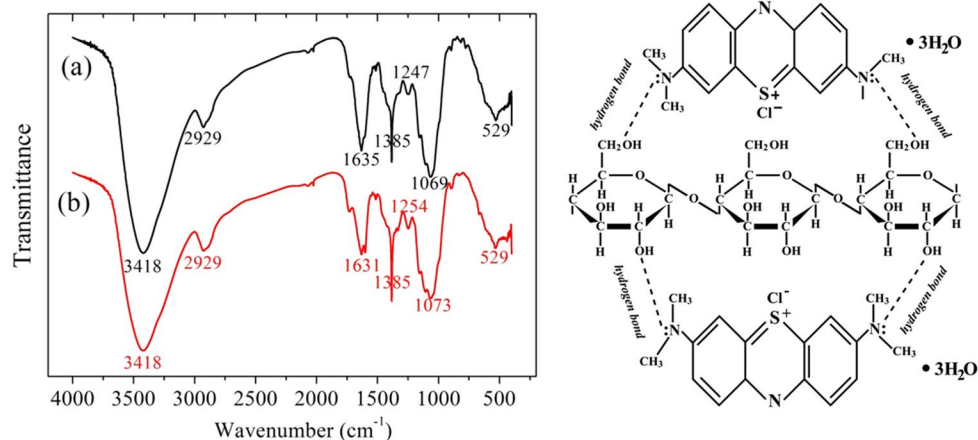
✉ Lin Zhu
lzhu@ujs.edu.cn

✉ Songjun Li
lsjchem@ujs.edu.cn

1 Institute of Polymer Materials, School of Materials Science and Engineering, Jiangsu University, 301 Xuefu Road, Zhenjiang 212013, People's Republic of China

Introduction

Water pollution was becoming more and more serious with the continuous improvement of the industrialization. Dye wastewater pollution, heavy metal wastewater pollution, refractory organic wastewater pollution, and other prominent water pollution problems had caused serious impact

on human living environment and ecosystem (Gwenzi et al. 2017). In some developed industrial areas, especially heavy industry and chemical industry, industrial wastewater emissions had greatly exceeded the capacity of local water environment (Rafatullah et al. 2010). The rapid development of dye industry had brought us a colorful world. However, the toxicity of synthetic dyes and the ecological and environmental problems caused by dye industry and overuse of dyes were also shocking. In addition to the dust caused by synthetic dyes that did harm to the health of workers, environmental pollution caused by synthetic dyes was mainly dye wastewater pollution.

Dye wastewater contained not only a large number of dye molecules, but also a lot of dye synthesis intermediates, dye synthesis additives, etc. So a certain amount of sulfonic acid, nitro, amino, chloride ions, and other aromatic derivatives widely existed in the dye wastewater. Meanwhile, it also contained a certain amount of mercury ions, chromium ions, zinc ions, fluoride ions, and other toxic heavy metal ions (Ali 2010). The pH value of the effluent dye wastewater varied greatly caused by the different dosage of acid and alkali due to different batches of dyes, different types of dyes, and different synthesis process of dyes, which brought some difficulties to the technology of wastewater treatment. In order to solve the problem of dye wastewater on environmental pollution, a large number of wastewater treatment methods began to emerge. These treatment methods could be roughly summed up as: chemical, biological, and physical methods (Khatri et al. 2015; Sivakumar et al. 2014). Chemical method could be divided into electrochemical method and advanced oxidation process. Biological method was the way to use the biological metabolism to change the organic matter in the wastewater into inorganic or various nutrients under the action of microorganisms. But these technologies and methods were limited by several obvious disadvantages such as operation costs, unsuitability for dispersed dyes, generated water products, and longer acclimatization phase. Physical treatment of dye wastewater involved the membrane separation technology, magnetic separation technology, and adsorption method, etc. Membrane separation technology was the way to separate the dye molecules using the selective permeability of the membrane. Magnetic separation technology was the way to use the magnetic field generated by the magnetic separator for separating. Adsorption method was the use of the mutual interaction between the adsorbents and dyes in the wastewater to achieve the purpose of removing pollutants. It was a physical process and would not destroy the molecular structure of the dye (Khatri et al. 2015; Sivakumar et al. 2014; Auta and Hameed 2014).

Adsorption method could selectively adsorb certain substances, especially for the decoloration of dyes. Among these water treatment methods, the adsorption method had more advantage than other removal techniques because of its simplicity, low cost, convenience, etc. (Bhatnagar and Sillanpää 2010). Therefore, adsorption method was a very good choice in the industry which was often used in the pretreatment or advanced treatment for printing and dyeing wastewater. The adsorption capacity depended on the type of adsorbent, so the low-cost adsorbent with high adsorption capacities was important and had gained great attention. There were many determinants for choosing different inexpensive adsorbents (Tang et al. 2012; Rafatullah et al. 2009). In recent years, some waste from the industrial, agricultural, and natural materials had received more and more attention because of its low prices. A large number of harmful substances from the wastewater could be absorbed by them. Many waste materials, such as longan shell (Wang et al. 2016), soya bean waste (Kooh et al. 2016), water bamboo leaves (Zhu et al. 2016), pulp and paper sludge (Chaukura et al. 2017a, b), pomelo peels (Zhu et al. 2017), durian shell (Wang et al. 2017), leaf-based cellulose (Zaidi et al. 2018), pomelo leaves (Lim et al. 2018), *Tremella fuciformis* (Zhu et al. 2018), and Jackfruit seed (Kooh et al. 2018), were used as adsorbent.

As a thiazine cationic dye, methylene blue (MB) was one of the most general water-soluble dyes used for industrial applications. It was frequently used in dyeing cotton, leather, silk, wools, printing, coloring paper, and coating for paper stock. It was also used in surgery as a sensitizer, diagnostics, and microbiology (Mitrogiannis et al. 2015). Because of its wide application, MB was considered as a common pollutant material in wastewater. Although it was not strongly toxic to human and animals, it could cause some negative effects, such as profuse sweating, an increased heart rate, diarrhea, gastritis, nausea and vomiting, mental confusion, tissue necrosis, shock (Abdallah and Taha 2012). Therefore, MB had been chosen in this study as a model molecule for basic dyes.

Bamboo, an ever green herbaceous plant, was widely cultivated in the tropical and subtropical regions, particularly in the East Asia (Lin et al. 2015). The young bamboo just grew out of the ground. It was called bamboo shoot with a height of 20–30 cm. Bamboo shoot had a high nutritional value, which was rich in protein, dietary fiber, and other nutrients. Bamboo shoot skin, as a by-product, was a prolific bioresource with an annual dry weight of 22 million tons in China. However, most of bamboo shoot skin was usually burned or discarded directly, which led to a large number of resource waste and serious environmental pollution every year. So the development and utilization of bamboo shoot skin could not only save resources, but also had an important impact on environmental protection (Li et al. 2015).

In this work, the bamboo shoot skin (BSS), as a low-cost and environment-friendly adsorbent, was utilized to remove MB from wastewater. This work included the assess of the influences of some related factors on the dye adsorption

process, such as the amount of adsorbent, the initial concentration of MB, the adsorption time and temperature, as well as the pH value of the solution. The BSS was also used as adsorbent to investigate the adsorption behavior for MB involved different kinetic, isotherm models, and thermodynamic parameters of the adsorption process.

Materials and methods

Materials

Bamboo shoot skin (BSS) was collected from the local supermarket in Zhenjiang, Jiangsu Province, China. All of the BSS was obtained from the same batch. To remove soluble impurities and dust, it was cleaned with distilled water and dried in a vacuum oven for 24 h at 60 °C. Then, it was shattered by grinder and sieved to obtain powder size range of 1–300 μm. After that, the particles were stored in the sealed glass container for future use. Prior to adsorption experiments, there were no other further physical or chemical treatments.

As the model adsorbate, methylene blue (MB) (Sinopharm Chemical Reagent Co. Ltd. Shanghai, China) was used as received without further purification. The chemical formula was $C_{16}H_{18}ClN_3S\cdot3H_2O$, and its molecular weight was 373.9 g/mol. NaOH or HCl was used to adjust the solution pH value. The pH meter (PHSJ-4F, Shanghai REX, China) was used to measure the pH value.

Characterization

The environmental scanning electron microscope (S-3400N) was utilized for studying the surface characteristics of samples. NEXUS 670 FTIR Spectrometer was utilized for obtaining the FTIR spectra of the BSS after and before adsorption of MB. The solid addition method (Dahri et al. 2015) was used to determine the point of zero charge of BSS.

Adsorption experiments

All adsorption experiments were conducted in conical flasks with capacity of 100 mL filled with 50 mL MB solution at constant magnetic stirring. The influence of adsorbent dosage (1–6 g/L), initial dye concentration (20–200 mg/L), adsorption time (5–240 min), temperature (20–70 °C), and initial pH value (3–12), were evaluated to study the adsorption efficiency of BSS. To separate the adsorbents from the liquid phase after finishing each adsorption procedure, the samples were centrifuged at 3000 rpm for 15 min. The MB concentration per adsorption experiment was tested by measuring the absorbance values with the spectrophotometer (Shimadzu UV-2550) at 666 nm. The amount of MB adsorbed at time t and percentage of MB removal could be obtained by the following equations, respectively:

$$Q_t = (C_0 - C_t) \times V/m \tag{1}$$

$$R(\%) = (C_0 - C_t)/C_0 \times 100 \tag{2}$$

where C_0 (mg L^{-1}) and C_t (mg L^{-1}) represent the dye concentration initially and at time t, respectively. V (L) was the solution volume, and m (g) was the adsorbent weight.

Results and discussion

Scanning electron microscope observation

The surface morphology of bamboo shoot skin was investigated by SEM, and the SEM photographs are shown in Fig. 1. It was seen that a large amount of irregular flaky
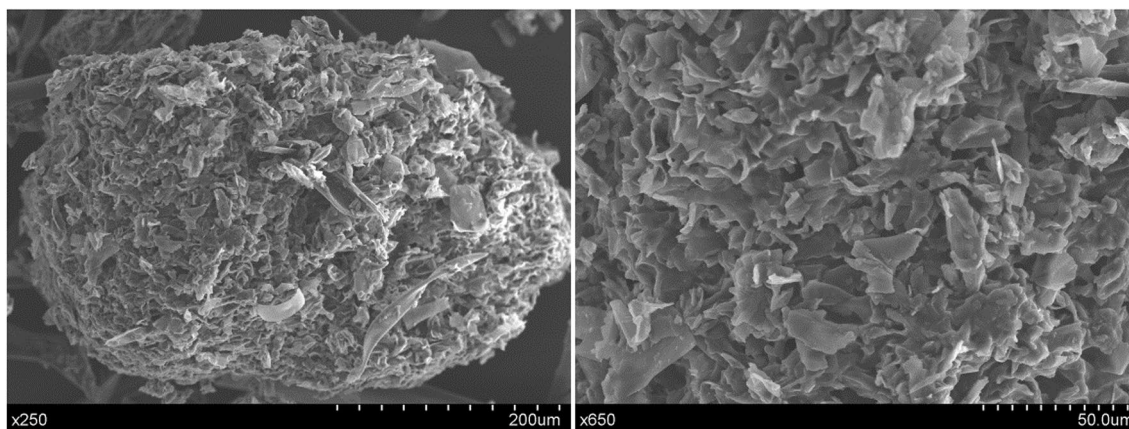

Fig. 1 SEM photographs of bamboo shoot skin at different magnifications

plant tissue stacked and curled up together, and there were also a large number of non-uniform pores existed in these layered structures, which presented large specific surface area. This structure provided a large amount of surface areas for contacting and adsorbing more dye molecules in the MB adsorption process (Lim et al. 2017).

Influence of adsorbent dosage

The dosage of adsorbent was a key technical parameter that greatly affected the removal of MB from wastewater because it determined the ability of the adsorbent which related to the number of adsorption sites (Doğan et al. 2007; Lim et al. 2015). At initial MB concentration 100 mg/L and adsorption time 60 min under ambient condition, the influence of variation of BSS dosage on the removal of MB is displayed in Fig. 2. As could be observed that the adsorption capacity of the BSS decreased and the dye removal rate increased when the BSS dosage enhanced.

When the dosage of adsorbent enhanced from 1 to 2 g/L, the adsorption capacity rapidly reduced from 32.64 to 21.27 mg/g, which reduced by 34.8%. The latter part of the reduction gradually stabilized, and the final adsorption capacity maintained at 12.4% mg/g. The results could be attributed to the fact that the mass of the BSS increased, while the adsorption capacity of the BSS was constant, and meanwhile the concentration of the dye was not changed, so the adsorption capacity of every unit was unsatisfied when the adsorbent dosage increased. In addition, on the one hand, the rapid decline from 1 to 2 g/L was also attributed to a marked raise in the amount of adsorbent. Then, the amount of adsorption reached equilibrium, and the decline tended to be flat. On the other hand, when the amount of adsorbent heightened from 1 to 3 g/L, the removal rate of MB enhanced from 32.64 to 56.85%, and the latter growth began to slow, reaching a maximum of 74.19%. The results could be attributed to the reason that the increase in the dose of BSS led to larger adsorption areas and more adsorption sites in the solution. The initial increase was due to the

relatively large increase in dose. When the adsorption did not reach saturation, the effect of subsequent additions on the removal efficiency reduced and the adsorption basically reached equilibrium.
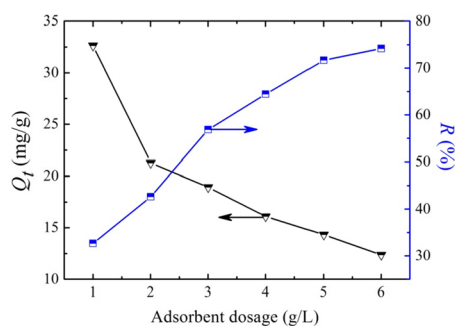
Influence of the initial concentrations

A large number of experimental results indicated that optimization of the initial concentration was important for adsorption studies of dye (Asfaram et al. 2014). Dye adsorption experiments with initial dye concentrations rose from 20 to 200 mg/L and were carried out at adsorbent dose of 2 g/L for 12 h under ambient condition.

Figure 3 displays the influence of initial concentrations of MB on the MB removal on BSS. The results displayed that the capacity of adsorption rose rapidly to 26.64 mg/g when the initial MB concentration enhanced from 20 to 100 mg/L. The latter part of the increase gradually stabilized which the adsorption capacity maintained at about 26.97 mg/g. These results indicated that the whole adsorption was basically balanced. On the other hand, when the initial MB concentration enhanced from 20 to 200 mg/L, the removal rate of MB reduced rapidly from 71.10 to 26.97% and the amplitude of the decrease gradually increased. Because the total amount of BSS in the solution remained constant, the contact of the MB with the BSS surface enhanced when the MB initial concentration increased. So the adsorption site on the surface of the BSS could be fully utilized, which was beneficial to the effect of the BSS on the MB adsorption. When the concentration of the solution increased to a certain extent, the adsorption of MB would not increase and maintained balance because the active site of the adsorbent in the system reached saturation (Lim et al. 2016).

Influence of adsorption time

Adsorption time was also an important parameter which could significantly describe adsorbent characteristics of the adsorption process (Mehmood et al. 2015). Therefore,
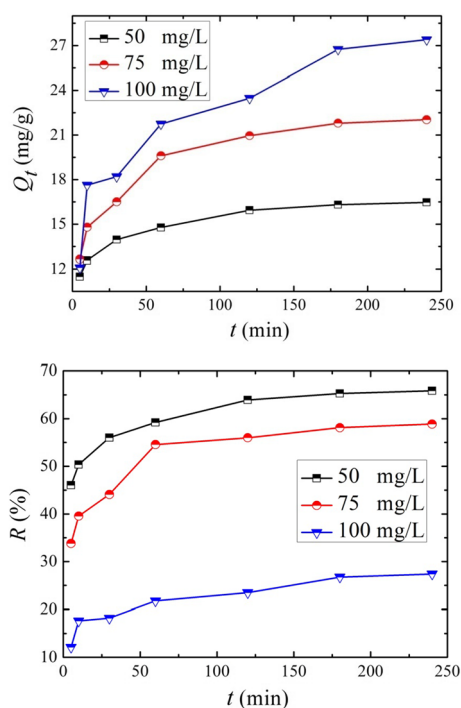
Fig. 2 The influence of adsorbent dosage on the removal of MB on BSS
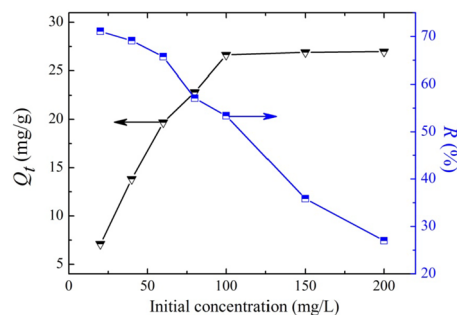
Fig. 3 The effect of initial MB concentrations on the removal of MB on BSS

the change of adsorption property with the adsorption time at three different MB concentrations (50 mg/L, 75 mg/L, 100 mg/L) was investigated at adsorbent dose of 2 g/L under ambient condition. Figure 4 displays the influence of adsorption time on the removal of MB on BSS. It could be observed that the capacity of adsorption and removal rate of MB both increased when the adsorption time increased under different dye concentrations. They raised greatly in the first 10 min. After that it increased slowly. Because the dye was mainly adsorbed on the outer surface of BSS at the initial stage of adsorption, the amount of adsorption first increased rapidly and then the speed of late adsorption gradually tended to be gentle. The initial rapid adsorption was due to the fact that the adsorption-driving force was the largest in the initial stage of adsorption because of the larger initial dye concentration and the more surface active sites. Then, the adsorbate gradually diffused within the micropores of the adsorbent, which resulted in the gradual increase in diffusion resistance. Meanwhile, the dye concentration gradually decreased. So the removal rate and adsorption capacity of MB increased slowly. The adsorption rate was mainly determined by diffusion resistance, which led to the slow adsorption rate. Moreover, the late adsorption was mainly adsorbed on the internal surface of the BSS, and the late low dye concentration and few surface active sites resulted in low adsorption-driving force, so the adsorption gradually slowed down and finally reached equilibrium.
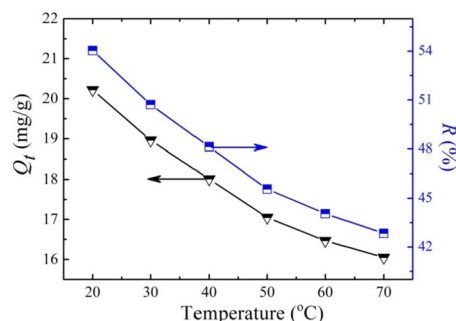
Influence of temperature

To explore the influence of temperatures on the adsorption behavior of BSS, the effects of different temperatures (20–70 °C) on adsorption experiments were investigated at initial MB concentration of 75 mg/L, adsorbent dose of 2 g/L, and adsorption time 60 min. Figure 5 shows the influence of temperature on the removal of MB on BSS. As displayed in Fig. 5, the adsorption capacity and removal rate of MB both reduced as the temperature enhanced from 20 to 70 °C. On the one hand, the adsorption of MB by the BSS was chemical adsorption. Because this type of adsorption was an exothermic process, it was harmful to the adsorption process by improving the adsorption temperature. On the other hand, the increase in the adsorption temperature made the thermal motion of the molecule become more intense, so it was less susceptible to the adsorption between MB and BSS. The results indicated that the adsorption experiments should be carried out at lower temperature (Han et al. 2008).

Influence of pH values of solution

The initial pH value of the sewage solution was also a key parameter during the adsorption process. It not only greatly influenced the ionization degree of the MB molecules and the surface charge of the adsorbent material, but also influenced the adsorption capacity of hydrogen ion and other ions (Kavitha and Namasivayam 2007). The influence of initial pH value ranged from 3 to 11.5 on the adsorption capacity was investigated at adsorbent dosage of 2 g/L, initial MB concentration of 75 mg/L, and the adsorption time of 12 h under ambient condition. As displayed in Fig. 6, the pH value had a significant influence on the adsorption capacity and removal rate of the cationic dye. The adsorption capacity and removal rate enhanced obviously with the increase in the pH value. This result was due to the effect of competition between hydrogen ions and cationic dyes. In the adsorption process, a large amount of hydrogen ions and cationic dye MB competed for limited active adsorption sites in the strong acid aqueous

Fig. 4 The influence of adsorption time on the removal of MB on BSS at three different concentrations of MB solution

Fig. 5 The influence of temperature on the removal of MB on BSS
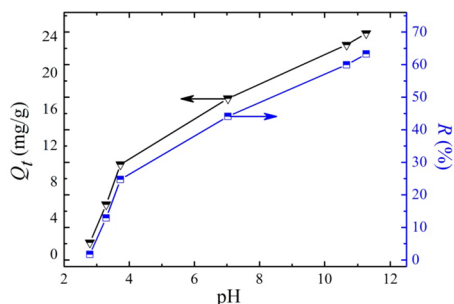
Fig. 6 The influence of pH values on the removal of MB on BSS

solution, so it would hinder the adsorption of cationic dye and reduce the adsorption capacity and removal rate. The influence of hydrogen ion concentration decreased when the pH value gradually increased. The effect gradually reduced until the positively charged cationic dye was adsorbed on the free binding site in the alkaline environment. So the adsorption capacity and removal rate obviously improved.

In addition, the point of zero charge of BSS was measured to be 7.3. This indicated that BSS obtained positive charge because of protonation of functional groups when the pH was lower than this value, resulting in electrostatic repulsion between dye cations and BSS. The negative charge existed on the surface of BSS when the pH was higher than this value, which resulted in electrostatic attraction. So the adsorption of cationic dye was favorable (Lim et al. 2017; Sadaf and Bhatti 2014).

Adsorption kinetics study

Adsorption was a well-known method of water purification, so it was necessary to obtain the equilibrium curve to demonstrate the adsorption kinetics of MB. Many adsorption kinetic models were utilized to study the adsorption mechanism. In this work, four kinetic models (pseudo-first-order model, pseudo-second-order model, intraparticle diffusion model, and Elovich kinetic model) were utilized to analyze the adsorption kinetics of MB molecules onto BSS.

These various models could be expressed as follows (Doğan et al. 2007; Asfaram et al. 2014; Ho and McKay 1999):

Pseudo-first order model: $\log \left(q_e - q_t\right) = \log q_e - \left(k_1/2.303\right)t$ (3)

Pseudo-second order model: $t/q_t = 1/\left(k_2 q_e^2\right) + t/q_e$ (4)
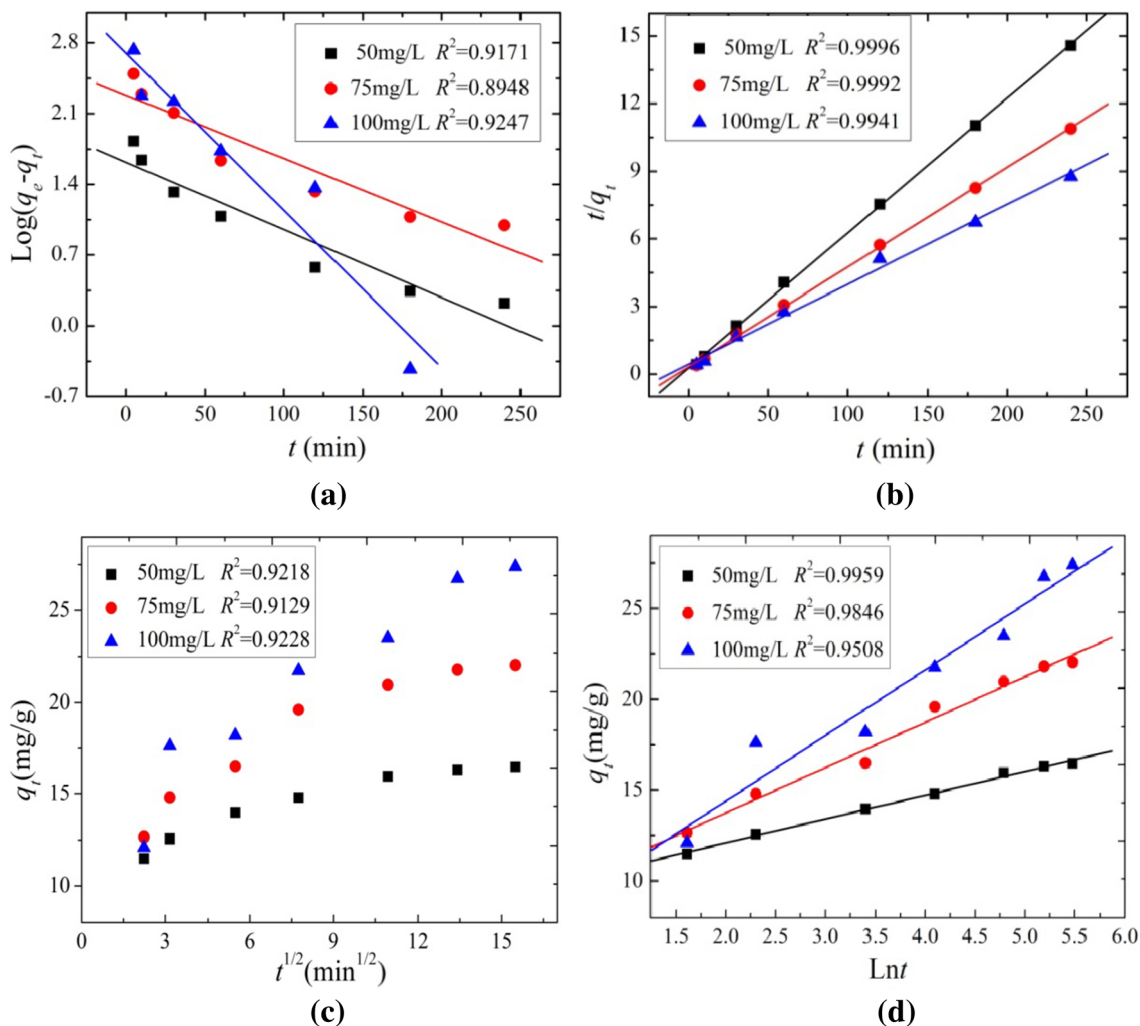
Intraparticle diffusion model: $q_t = k_d t^{1/2} + C$ (5)

Elovich kinetic model: $q_t = 1/\beta \ln\left(\alpha\beta\right) + 1/\beta \ln t$ (6)

The linear plots of $\log(q_e - q_t)$ versus t, t/q_t versus t, q_t versus $t^{1/2}$, and q_t versus $\ln t$ for three concentrations are displayed in Fig. 7a–d, and correlation coefficients obtained from the slope and intercept of the plots are listed in Table 1. It could be observed that as the concentration enhanced from 50 to 100 mg/L, the correlation coefficients (R^2) for pseudo-first-order kinetic model were 0.9171, 0.8948, and 0.9247, respectively, the R^2 for pseudo-second-order kinetic model were 0.9996, 0.9992, and 0.9941, respectively, the R^2 for intraparticle diffusion kinetic model were 0.9218, 0.9129, and 0.9228, respectively, and the R^2 for Elovich kinetic model were 0.9959, 0.9846, and 0.9508, respectively. It could be obtained that the kinetic data showed the best fit to the pseudo-second-order model with higher R^2 which were higher than 0.99 at the three different concentrations. The q_e values obtained by the model were very approximative to the q_e values obtained from the experiment, which demonstrated the applicability of the pseudo-second-order kinetic model to follow the adsorption process of the MB onto the BSS. On the contrary, the other three models were not very applicable. For example, the obtained q_e values obtained from the linear plots in pseudo-first-order model did not correspond with the experimental q_e values. The values of C were much larger than zero in intraparticle diffusion model, indicating that the increase in the concentration of dye promoted the boundary layer diffusion effect. The constants α and β decreased in the Elovich kinetic model indicated that the chemical adsorption rate and the available adsorption surface would be reduced (Mehmood et al. 2015).

Adsorption isotherms

The equilibrium adsorption isotherm was significant in investigating the interactive behavior between adsorbate and adsorbent, and it also had an important part in optimizing the use of adsorbents. The main parameters calculated from the different adsorption isotherms gave essential information about the adsorbent and the adsorbate. Langmuir and Freundlich isotherm models were the most frequently used adsorption isotherms in the study of the adsorption process (Kumar and Sivanesan 2006).

The Langmuir isotherm model was based on the adsorption of monomolecular layers. The Langmuir model assumed that the adsorbent surface was homogeneous and adsorbent surface had the same adsorption capacity. When the adsorbate reached the saturated state on the adsorbent surface, the adsorption capacity reached the maximum value. There was no transfer movement on the adsorbent surface when the saturated state reached. In the dynamic equilibrium, the adsorption rate and desorption rate of the adsorbate on the adsorbent were the same. The relationship between the equilibrium adsorption capacity q_m and the solution equilibrium concentration C_e in the Langmuir equation was as follows:

Fig. 7 **a** Pseudo-first-order kinetic model plot, **b** pseudo-second-order kinetic model plot, **c** intraparticle diffusion model plot, and **d** Elovich kinetic model plot for the adsorption of MB by BSS

Table 1 Kinetic parameters for adsorption of MB onto BSS

Kinetic model	Parameters	Dye concentration (mg/L)		
		50	75	100
Experiment value	$q_{e,exp}$ (mg/g)	17.72	24.74	27.39
Pseudo-first-order	$q_{e,cal}$ (mg/g)	5.05	9.81	14.84
	k_1 (min^{-1})	0.0154	0.0144	0.0358
	R^2	0.9171	0.8948	0.9247
Pseudo-second-order	$q_{e,cal}$ (mg/g)	16.72	22.61	28.25
	k_2 (g mg^{-1} min^{-1})	0.0125	0.00597	0.00278
	h (mg g^{-1} min^{-1})	3.49	3.05	2.22
	R^2	0.9996	0.9992	0.9941
Intraparticle diffusion	Intercept C	11.46	12.54	12.46
	k_d (mg g^{-1} min$^{-0.5}$)	0.3635	0.6939	1.0248
	R^2	0.9218	0.9129	0.9228
Elovich	α (mg g^{-1} min^{-1})	1812.6	82.9	26.2
	β (g/mg)	0.7635	0.4004	0.2766
	R^2	0.9959	0.9846	0.9508

$$C_e/q_e = C_e/q_m + 1/K_L q_m \tag{7}$$

The separation factor R_L could be obtained from the following equation using the parameter K_L in the Langmuir model:

$$R_L = (1 + K_L C_0)^{-1} \tag{8}$$

If R_L value was equal to zero, it indicated the type of adsorption was irreversible. If R_L value was between 0 and 1, it indicated the type of adsorption was favorable. If R_L value was equal to 1, it indicated the type of adsorption was linear. If R_L value was greater than 1, it indicated the type of adsorption was unfavorable ($R_L > 1$). In this study, the R_L value was between 0.058 and 0.38, implying that the adsorption process was favorable.

The Freundlich isotherm model was an empirical formula for the nonlinear model. Compared with the Langmuir equation, it was suitable for the condition of

inhomogeneous surface, which had advantages in describing the adsorption of high concentration adsorbate, and it was generally not well used for low concentration adsorbate. The linear form of Freundlich equation was expressed as follows:

$$\ln q_e = \ln K_F + 1/n \ln C_e \tag{9}$$

In the above equation, K_F was the Freundlich adsorption coefficient and n was the Freundlich constant. It was generally believed that adsorbate tended to be adsorbed easily on the adsorbent surface when the $1/n$ value was less than 1.0. But when the $1/n$ value was more than 1.0, it was difficult to absorb and illustrated the adsorption process was chemical biosorption mechanism. K_F and n could be obtained from the linear plot of $\ln q_e$ versus $\ln C_e$. In this study, the n value was 2.54, which indicated that the adsorption was favorable. This result was identical with the results obtained from the Langmuir model.

The plots of the two isotherms are shown in Fig. 8a, b, and Table 2 lists the correlation coefficients. It could be concluded that the equilibrium data were fitted well by Langmuir isotherm model because of higher correlation coefficients and the plot of C_e/q_e versus C_e also showed straight line. However, the experimental data did not show good fit to the Freundlich isotherm model because of its low R^2 value and it also showed bad linearity between $\ln C_e$ and $\ln q_e$.

Thermodynamic parameters

It was essential to investigate the thermodynamic behavior of an adsorption behavior, because the corresponding parameters of thermodynamic could determine whether the process was spontaneous or not. In this work, thermodynamic study of adsorption of MB on BSS was investigated

Table 2 Isotherm parameters and correlation coefficients calculated for the adsorption of MB onto BSS

Langmuir			Freundlich		
q_m (mg/g)	K_L (L/mg)	R^2	K_F (mg/g) (L/mg)$^{1/n}$	n	R^2
29.88	0.0812	0.9933	4.84	2.54	0.8137

between 20 and 70 °C at original MB concentration of 75 mg/L and adsorbent amount of 2 g/L. Thermodynamic parameters, including the Gibbs free energy change ($\Delta G°$), enthalpy ($\Delta H°$), and entropy ($\Delta S°$), were important for specific application of an adsorbent. The thermodynamic parameters could be obtained using the rate equation and the van't Hoff equation which could be expressed as:

$$K_d = q_e/C_e \tag{10}$$

$$\Delta G° = -RT \ln K_d \tag{11}$$

$$\Delta G° = \Delta H° - T\Delta S° \tag{12}$$

$$\ln K_d = (\Delta S°/R) - (\Delta H°/RT) \tag{13}$$

where K_d represents the standard thermodynamic equilibrium constant, q_e represents the amount of dye adsorbed on the adsorbent at equilibrium, C_e represents the equilibrium concentration of dye in the solution, R was the gas constant, and T was the absolute temperature. The values of $\Delta H°$ and $\Delta S°$ could be estimated from the slopes and intercepts which determined by plotting $\ln K_d$ versus $1/T$. The plot is shown in Fig. 9. Table 3 lists the relevant values of $\Delta G°$, $\Delta H°$, and $\Delta S°$. It showed that the values of all $\Delta G°$ were negative, implying the feasibility of the adsorption process and the spontaneous nature. Furthermore, the increase in $\Delta G°$ with the increase in temperature indicated the adsorption was
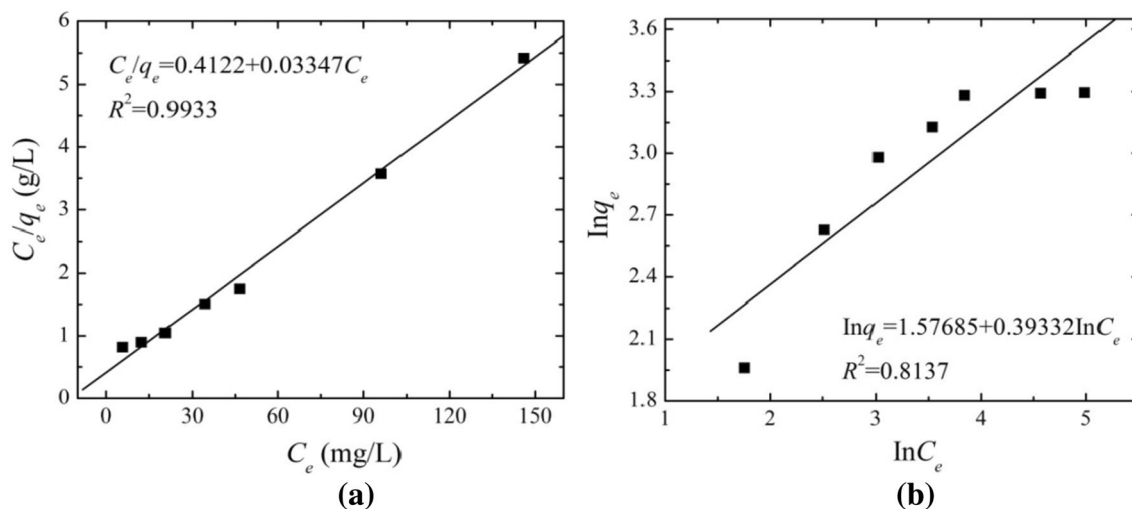
Fig. 8 **a** Langmuir isotherm models plot and **b** Freundlich isotherm models plot for the adsorption of MB by BSS
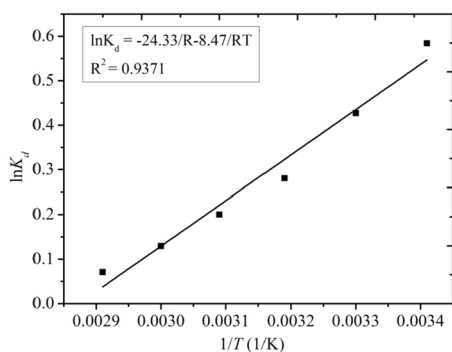
Fig. 9 Plot of $\ln K_d$ versus $1/T$ for the adsorption of MB on BSS

Table 3 Thermodynamic parameters for the adsorption of MB onto BSS

Temperature (K)	$\Delta G°$ (KJ/mol)	$\Delta H°$ (KJ/mol)	$\Delta S°$ (J/mol/K)
293.15	−1.33	−8.47	−24.33
303.15	−1.09		
313.15	−0.85		
323.15	−0.61		
333.15	−0.36		
343.15	−0.12		

exothermic and more favorable at low temperatures. Negative $\Delta H°$ and $\Delta S°$ values indicated exothermic reaction and the decreased randomness at the interface of BSS and MB solution, respectively (Fathi et al. 2015).

Adsorption mechanism

The elucidation of the adsorption mechanism was relatively difficult in adsorption studies. First, the structure and properties of two substances involved in the adsorption process should be clearly explicit. For adsorbate, methylene blue was a cationic dye with two amino groups, which dissociated into MB^+ and Cl^- ions in aqueous solution. For the adsorbent, BSS had a porous surface which could be observed from SEM images as shown in Fig. 1. Then, the surface functional groups and chemical bonds of the BSS which was the key effects on its adsorption properties should be studied. Therefore, FTIR technique was used to illuminate these groups and bonds, and the FTIR spectrum of GFP is illustrated in Fig. 10. The strong and broadband stretch located at 3418 cm^{-1} indicated the appearance of O–H groups of cellulose, hemicellulose, lignin, and pectin in BSS. The narrow band located at 1385 cm^{-1} and the weak band located at 2929 cm^{-1}, which were well-defined peaks, were assigned to the bending vibration and stretching vibration of asymmetric or symmetric C–H of aliphatic acids, respectively. The band located at 1635 cm^{-1} was assigned to stretching vibrations of carbonyl groups on aldehydes
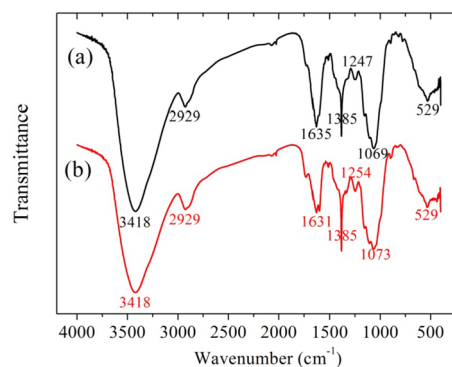

Fig. 10 FTIR spectra of BSS (a) before and (b) after the adsorption of MB

and ketones, while the small band located at 1247 cm^{-1} was assigned to the stretching formation of –OH and deformation vibration of C=O of carboxylic acids and phenols. The other strong band located at 1069 cm^{-1} was assigned to C–O–C functional group stretching of the cellulose and lignin structures in BSS (Sadaf and Bhatti 2014).

The above FTIR spectrum analysis showed that the BSS contained many hydroxyl and carboxyl groups. Based on the above experimental results and the structure and properties of adsorbate and adsorbent, the process of adsorption of MB by BSS included the following steps. First, the molecules of MB migrated from the aqueous solution to the BSS surface. Second, the MB molecules passed through the boundary layer between the aqueous solution and the BSS and reached the BSS surface. Third, the functional groups of BSS interacted with the MB molecules, so that the MB molecules were adsorbed onto the BSS. The interaction included hydrogen bonds formed by hydroxyl groups on the surface of BSS and nitrogen atoms of MB molecules, which are exhibited in Fig. 11. The interaction might also include ion exchange process between hydrogen ions and dyes, which was demonstrated as:

$$BSS−OH \rightleftharpoons BSS−O^- + H^+$$

$$BSS−O^- + MB^+ \rightleftharpoons BSS−O−MB + H^+$$
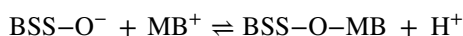
In addition, the carboxylic groups on the surface of BSS formed negatively charged carboxylate ligands after the carboxylic groups were deprotonated at pH above 4 (Aguayo-Villarreal et al. 2013). The carboxylate ligands interacted with the positively charged MB molecules, which were demonstrated as:
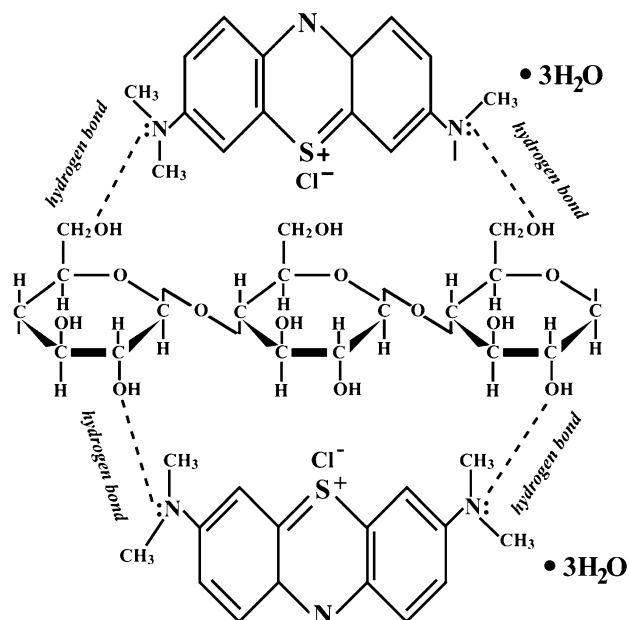
$$BSS−COOH \rightleftharpoons BSS−COO^- + H^+$$

$$BSS−COO^- + MB^+ \rightleftharpoons BSS−COO−MB + H^+$$
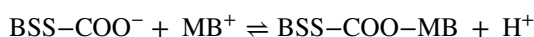
Fig. 11 Adsorption mechanism of MB onto BSS

At last, MB molecules diffused in the inner pore of the BSS.

Comparison of BSS with other adsorbents

The absorption ability of BSS had been compared with other adsorbents previously utilized for adsorption of MB. Table 4 compares the adsorption capacities (the maximum monolayer adsorption) of the BSS with other adsorbents. It displayed that the adsorption amount of MB on BSS was comparable with some previously reported adsorbents, but lower than some adsorbents. However, bamboo shoot skin

was cheap, easy to obtain, sustainable, and friendly to environment as an agricultural waste. As an adsorbent, it could make the waste into valuable resources without secondary pollution and realized the comprehensive utilization of resources, which would benefit economy, environment, and society.

Conclusions

In conclusion, bamboo shoot skin could be utilized as an adsorbent to adsorb MB from sewage. The bamboo shoot skin displayed high efficiency to adsorb MB from sewage. The adsorption efficiency of BSS was displayed to be affected by many operational parameters. The maximum adsorption capacity was 29.88 mg/g. Four kinetic models were utilized to investigate the kinetic study of MB onto BSS, and the results indicated that the pseudo-second-order kinetic model could well describe the adsorption kinetics. In addition, two isotherm models were applied to study the adsorption behavior of MB onto BSS, and the equilibrium process was better followed by the Langmuir isotherm model than Freundlich isotherm model. The calculated thermodynamic parameters indicated the spontaneous nature and the feasibility of the adsorption process. The maximum MB adsorption capacity of BSS was comparable with some previously reported adsorbents, but lower than some adsorbents. These results indicated that the BSS could be very promising adsorbent.

Table 4 Comparison of MB adsorption capacity of BSS with other adsorbents

Adsorbent	Amount adsorbed (mg/g)	References
Banana peel	18.65	(Amela et al. 2012)
Jute processing waste	22.47	(Banerjee and Dastidar 2005)
Raw ball clay	34.65	(Auta and Hameed 2012)
Clay	58.20	(Gürses et al. 2006)
Glass fibers	2.24	(Chakrabarti and Dutta 2005)
Coal fly ash	16.60	(Wang et al. 2008)
Coconut coir	15.59	(Sharma and Upadhyay 2009)
Peat of Brunei Darussalam IV	143.96 (0.45 mmol g^{-1})	(Chieng et al. 2014)
Artocarpus odoratissimus skin	184.60 (0.58 mmol g^{-1})	(Lim et al. 2015)
Casuarina equisetifolia needle	110.80	(Dahri et al. 2015)
Dragon fruit skin	640	(Priyantha et al. 2015)
Breadnut core	369	(Lim et al. 2016)
Breadnut peel	409	(Lim et al. 2017)
Bamboo shoot skin	29.88	This work

References

Abdallah R, Taha S (2012) Biosorption of methylene blue from aqueous solution by nonviable *Aspergillus fumigatus*. Chem Eng J 195:69–76

Aguayo-Villarreal IA, Ramírez-Montoya LA, Hernández-Montoya V, Bonilla-Petriciolet A, Montes-Moránc MA, Ramírez-López EM (2013) Sorption mechanism of anionic dyes on pecan nut shells (*Carya illinoinensis*) using batch and continuous systems. Ind Crop Prod 48:89–97

Ali H (2010) Biodegradation of synthetic dyes—a review. Water Air Soil Pollut 213(1–4):251–273

Amela K, Hassen MA, Kerroum D (2012) Isotherm and kinetics study of biosorption of cationic dye onto banana peel. Energy Procedia 19:286–295

Asfaram A, Fathi MR, Khodadoust S, Naraki M (2014) Removal of Direct Red 12B by garlic peel as a cheap adsorbent: kinetics, thermodynamic and equilibrium isotherms study of removal. Spectrochim Acta A 127:415–421

Auta M, Hameed BH (2012) Modified mesoporous clay adsorbent for adsorption isotherm and kinetics of methylene blue. Chem Eng J 198:219–227

Auta M, Hameed BH (2014) Chitosan–clay composite as highly effective and low-cost adsorbent for batch and fixed-bed adsorption of methylene blue. Chem Eng J 237:352–361

Banerjee S, Dastidar MG (2005) Use of jute processing wastes for treatment of wastewater contaminated with dye and other organics. Bioresour Technol 96(17):1919–1928

Bhatnagar A, Sillanpää M (2010) Utilization of agro-industrial and municipal waste materials as potential adsorbents for water treatment—a review. Chem Eng J 157(2):277–296

Chakrabarti S, Dutta BK (2005) On the adsorption and diffusion of methylene blue in glass fibers. J Colloid Interface Sci 286(2):807–811

Chaukura N, Murimba EC, Gwenzi W (2017a) Sorptive removal of methylene blue from simulated wastewater using biochars derived from pulp and paper sludge. Environ Technol Innov 8:132–140

Chaukura N, Murimba EC, Gwenzi W (2017b) Synthesis, characterisation and methyl orange adsorption capacity of ferric oxide–biochar nano-composites derived from pulp and paper sludge. Appl Water Sci 7:2175–2186

Chieng HI, Zehra T, Lim LBL, Priyantha N, Tennakoon DTB (2014) Sorption characteristics of peat of Brunei Darussalam IV: equilibrium, thermodynamics and kinetics of adsorption of methylene blue and malachite green dyes from aqueous solution. Environ Earth Sci 72:2263–2277

Dahri MK, Kooh MRR, Lim LBL (2015) Application of *Casuarina equisetifolia* needle for the removal of methylene blue and malachite green dyes from aqueous solution. Alex Eng J 54:1253–1263

Doğan M, Özdemir Y, Alkan M (2007) Adsorption kinetics and mechanism of cationic methyl violet and methylene blue dyes onto sepiolite. Dyes Pigments 75(3):701–713

Fathi MR, Asfaram A, Farhangi A (2015) Removal of Direct Red 23 from aqueous solution using corn stalks: isotherms, kinetics and thermodynamic studies. Spectrochim Acta A 135:364–372

Gürses A, Doğar Ç, Yalçın M, Açıkyıldız M, Bayrak R, Karaca S (2006) The adsorption kinetics of the cationic dye, methylene blue, onto clay. J Hazard Mater 131(1):217–228

Gwenzi W, Chaukura N, Noubactep C, Mukome FND (2017) Biochar-based water treatment as a potential low-cost and sustainable technology for clean water provision. J Environ Manag 197:732–749

Han R, Ding D, Xu Y, Zou W, Wang Y, Li Y, Zou L (2008) Use of rice husk for the adsorption of congo red from aqueous solution in column mode. Bioresour Technol 99(8):2938–2946

Ho YS, McKay G (1999) Pseudo-second order model for sorption processes. Process Biochem 34(5):451–465

Kavitha D, Namasivayam C (2007) Experimental and kinetic studies on methylene blue adsorption by coir pith carbon. Bioresour Technol 98(1):14–21

Khatri A, Peerzada MH, Mohsin M, White M (2015) A review on developments in dyeing cotton fabrics with reactive dyes for reducing effluent pollution. J Clean Prod 87:50–57

Kooh MRR, Dahri MK, Lim LBL, Lim LH, Malik OA (2016) Batch adsorption studies of the removal of methyl violet 2B by soya bean waste: isotherm, kinetics and artificial neural network modeling. Environ Earth Sci 75:783

Kooh MRR, Dahri MK, Lim LBL (2018) Jackfruit seed as low-cost adsorbent for removal of malachite green: artificial neural network and random forest approaches. Environ Earth Sci 77:434

Kumar KV, Sivanesan S (2006) Equilibrium data, isotherm parameters and process design for partial and complete isotherm of methylene blue onto activated carbon. J Hazard Mater 134(1):237–244

Li L, Xu J, Mu Y, Han L, Liu R, Cai Y, Huang X (2015) Chemical characterization and anti-hyperglycaemic effects of polyphenol enriched longan (*Dimocarpus longan* Lour.) pericarp extracts. J Funct Foods 13:314–322

Lim LBL, Priyantha N, Ing CH, Dahri MK, Tennakoon DTB, Zehra T, Sukleung M (2015) *Artocarpus odoratissimus* skin as potential low-cost biosorbent for the removal of methylene blue and methyl violet 2B. Desalin Water Treat 53:964–975

Lim LBL, Priyantha N, Chieng HI, Dahri MK (2016) *Artocarpus camansi* Blanco (Breadnut) core as low-cost adsorbent for the removal of methylene blue: equilibrium, thermodynamics and kinetics studies. Desalin Water Treat 57:5673–5685

Lim LBL, Priyantha N, Tennakoon DTB, Chieng HI, Dahri MK, Suklueng M (2017) Breadnut peel as a highly effective low-cost biosorbent for methylene blue: equilibrium, thermodynamic and kinetic studies. Arab J Chem 10:S3216–S3228

Lim LBL, Priyantha N, Lu YC, Zaidi NAHM (2018) Effective removal of methyl violet dye using pomelo leaves as a new low-cost adsorbent. Desalin Water Treat 110:264–274

Lin Y, Lin Y, Lin H, Zhang S, Chen Y, Shi J (2015) Inhibitory effects of propyl gallate on browning and its relationship to active oxygen metabolism in pericarp of harvested longan fruit. LWT Food Sci Technol 60(2):1122–1128

Mehmood A, Bano S, Fahim A, Parveen R, Khurshid S (2015) Efficient removal of crystal violet and eosin B from aqueous solution using *Syzygium cumini* leaves: a comparative study of acidic and basic dyes on a single adsorbent. Korean J Chem Eng 32(5):882–895

Mitrogiannis D, Markou G, Çelekli A, Bozkurt H (2015) Biosorption of methylene blue onto *Arthrospira platensis* biomass: kinetic, equilibrium and thermodynamic studies. J Environ Chem Eng 3:670–680

Priyantha N, Lim LBL, Dahri MK (2015) Dragon fruit skin as potential biosorbent for the removal of methylene blue dye from aqueous solution. Int Food Res J 22:2141–2148

Rafatullah M, Sulaiman O, Hashim R, Ahmad A (2009) Adsorption of copper (II): chromium (III): nickel (II) and lead (II) ions from aqueous solutions by meranti sawdust. J Hazard Mater 170(2):969–977

Rafatullah M, Sulaiman O, Hashim R, Ahmad A (2010) Adsorption of methylene blue on low-cost adsorbents: a review. J Hazard Mater 177(1):70–80

Sadaf S, Bhatti HN (2014) Evaluation of peanut husk as a novel, low cost biosorbent for the removal of Indosol Orange RSN dye from aqueous solutions: batch and fixed bed studies. Clean Technol Environ Policy 16:527–544

Sharma YC, Upadhyay SN (2009) Removal of a cationic dye from wastewaters by adsorption on activated carbon developed from coconut coir. Energy Fuel 23(6):2983–2988

Sivakumar A, Murugesan B, Loganathan A, Sivakumar P (2014) A review on decolourisation of dyes by photodegradation using various bismuth catalysts. J Taiwan Inst Chem Eng 45(5):2300–2306

Tang H, Zhou W, Zhang L (2012) Adsorption isotherms and kinetics studies of malachite green on chitin hydrogels. J Hazard Mater 209:218–225

Wang S, Ma Q, Zhu ZH (2008) Characteristics of coal fly ash and adsorption application. Fuel 87(15):3469–3473

Wang Y, Zhu L, Jiang HT, Hu F, Shen XQ (2016) Application of longan shell as non-conventional low-cost adsorbent for the removal of cationic dye from aqueous solution. Spectrochim Acta A 159:254–261

Wang Y, Zhu L, Zhu FY, You LJ, Shen XQ, Li SJ (2017) Removal of organic solvents/oils using carbon aerogels derived from waste durian shell. J Taiwan Inst Chem E 78:351–358

Zaidi NAHM, Lim LBL, Usman A (2018) *Artocarpus odoratissimus* leaf-based cellulose as adsorbent for removal of methyl violet and crystal violet dyes from aqueous solution. Cellulose 25:3037–3049

Zhu L, Wang Y, He TT, You LJ, Shen XQ (2016) Assessment of potential capability of water bamboo leaves on the adsorption removal efficiency of cationic dye from aqueous solutions. J Polym Environ 24:148–158

Zhu L, Wang Y, Wang YX, You LJ, Shen XQ, Li SJ (2017) An environmentally friendly carbon aerogels derived from waste pomelo peels for the removal of organic pollutants/oils. Mesoporous Mesoporous Mater 241:285–292

Zhu L, Wang Y, Zhu FY, You LJ, Shen XQ (2018) Evaluation of the biosorption characteristics of *Tremella fuciformis* for the decolorization of cationic dye from aqueous solution. J Polym Environ 26:1051–1060